Molecular Cell, Vol. 5, 889–895, May, 2000, Copyright ©2000 by Cell Press

Structure of BamHI Bound to Nonspecific DNA: A Model for DNA Sliding

Hector Viadiu*† and Aneel K. Aggarwal†‡
*Department of Biochemistry and Molecular Biophysics
Columbia University
New York, New York 10032
†Structural Biology Program
Department of Physiology and Biophysics
Mount Sinai School of Medicine
New York, New York 10029

Summary

The central problem faced by DNA binding proteins is how to select the correct DNA sequence from the sea of nonspecific sequences in a cell. The problem is particularly acute for bacterial restriction enzymes because cleavage at an incorrect DNA site could be lethal. To understand the basis of this selectivity, we report here the crystal structure of endonuclease BamHI bound to noncognate DNA. We show that, despite only a single base pair change in the recognition sequence, the enzyme adopts an open configuration that is on the pathway between free and specifically bound forms of the enzyme. Surprisingly, the DNA drops out of the binding cleft with a total loss of base-specific and backbone contacts. Taken together, the structure provides a remarkable snapshot of an enzyme poised for linear diffusion (rather than cleavage) along the DNA.

Introduction

In recent years, there has been an explosion in the number of three-dimensional structures of proteins bound to their target DNA sequence (Harrison and Aggarwal, 1990; Pabo and Sauer, 1992). This affluence of information has helped to increase our understanding of how proteins recognize a specific DNA sequence. However, our understanding of protein–DNA recognition will be incomplete unless we can also describe how proteins are nonspecifically bound to DNA (von Hippel, 1994). This gap in our knowledge has been partly filled by thermodynamic studies that point to a distinct conformational state for the nonspecific complex (Mossing and Record, 1985; von Hippel and Berg, 1986). Nonspecific complexes are thought to be more hydrated at the protein–DNA interface (Garner and Rau, 1995; Sidorova and Rau, 1996), stabilized primarily through electrostatic interactions (deHaseth et al., 1977; Revzin and von Hippel, 1977), and exhibit a low heat capacity change on binding (Takeda et al., 1992; Ladbury et al., 1994). Together, these features lend themselves well to sliding along the DNA (von Hippel and Berg, 1989).

The problem of specific versus nonspecific DNA selection is particularly acute for the bacterial restriction enzymes (Roberts and Halford, 1993). For instance, for every BamHI cognate DNA site (GGATCC) in the *B. amyloliquefaciens* H genome, there are ~18 sites that differ by only a single base pair. Only the cognate sites are protected from cleavage by methylation produced by the partner methylase enzyme (Roberts and Halford, 1993). Restriction enzymes have thus evolved stringent specificity for their recognition sequence, such that even a single base pair change can reduce their cleavage activity by over a million-fold (Lesser et al., 1990; Thielking et al., 1990). To understand the basis of this selectivity, we have structurally characterized BamHI at different stages of its catalytic pathway. We have previously reported structures of BamHI bound to its cognate site and in the absence of DNA (Newman et al., 1994, 1995). Together, these structures reveal the conformational changes that occur on specific DNA binding, including rotation of subunits and the folding of disordered regions. The most striking conformational change is the unraveling of C-terminal α helices to form partially disordered "arms" (Newman et al., 1995). However, the critical structure that has been missing for a complete understanding of this selectivity is the nonspecific complex. We report here the structure of BamHI bound to a noncognate DNA sequence (GAATCC) that differs by only a single base pair from the cognate (G*G*ATCC) sequence. The structure reveals the enzyme in a distinct conformation that is incompetent for cleavage but competent for sliding (Figure 1).

Results and Discussion

Structure Determination

The nonspecific cocrystals were grown from solutions containing equimolar amounts of BamHI dimer and the nonspecific DNA 5′-ATGAATCCATA-3′. An important factor in obtaining these crystals was the lowering of salt concentration in the protein buffer from 0.5 to 0.05 M NaCl (Viadiu et al., 2000). The structure was solved by molecular replacement using a truncated BamHI subunit from the specific complex as the initial search model. The DNA was difficult to locate initially but became better defined as the refinement progressed. The final model was refined to 1.9 Å resolution and contains most of the protein (residues 1–209 out of total 213 for one monomer and residues 1–212 for the other monomer), 8 out 11 DNA base pairs, and 579 water molecules (Table 1). Figure 1B shows electron density for the DNA in a $|F_o| - |F_c|$ simulated annealing omit map.

BamHI Forms a Loose, Dynamic Complex with Nonspecific DNA

The noncognate DNA is accommodated loosely within a cleft at the bottom of the BamHI dimer (Figure 1). The DNA protrudes out of the cleft, whereas, in the specific complex, it is almost surrounded by the enzyme (Figure 2). The two-fold symmetry of BamHI coincides with the approximate two-fold axis of the DNA (Figure 3). However, compared to the specific complex, the enzyme

‡To whom correspondence should be addressed (e-mail: aggarwal@inka.mssm.edu).

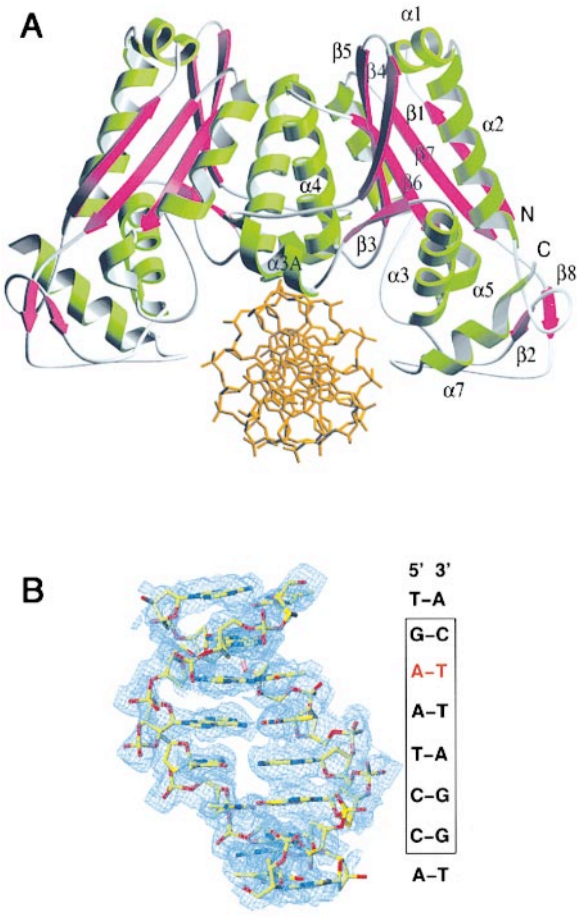

Figure 1. BamHI Bound to Nonspecific DNA

(A) The structure viewed down the DNA axis. The α helices are colored in green, the β strands in purple, and the DNA in orange. Only one subunit is labeled. N and C mark the N and C termini of the protein.

(B) A $|F_o| - |F_c|$ simulated annealing omit map calculated in the absence DNA. The map returns the electron densities for 8 of the 11 base pairs of the DNA. The DNA sequence is shown alongside the electron density, with the single base pair mutation marked in red.

Table 1. Crystallographic Analysis

Data	Rotating Anode	CHESS-1	CHESS-2
Wavelength (Å)	1.54	0.91	0.91
Resolution (Å)	2.5	2.0	1.9
Unique reflections	23,995	30,332	53,008
Completeness (%)	99.4 (98.4)[a]	68.0 (47.6)	96.1 (85.2)
R_{merge}[b] (%)	8.2 (28.0)	11.1 (32.2)	5.7 (28.4)
Refinement Statistics (10–1.9 Å)			
Reflections			51,166
R_{factor} (%)			19.1
R_{free}[c] (%)			23.0
Total number of atoms			4317
Number of waters			579
Rms bond lengths			0.009
Rms bond angles			1.48
Mean B value, overall (Å^2)			34.1
Mean B value, protein (Å^2)			28.5
Mean B value, DNA (Å^2)			73.6
Mean B value, solvent (Å^2)			45.3

[a] The numbers in parentheses refer to the last resolution shells.
[b] $R_{merge} = \Sigma|I_{obs} - \langle I \rangle|/\Sigma\langle I \rangle$, calculated for all data.
[c] Calculated with the 5% of the reflection data excluded from refinement.

is tilted about this axis by ~20°, resulting in markedly different DNA binding surfaces in the two complexes (Figures 2 and 3). Moreover, in the nonspecific complex, the DNA binding cleft is widened by an outward symmetrical motion of the BamHI monomers (R and L), such that the distance across the cleft increases from 20 Å to 25 Å. Correspondingly, the buried solvent-accessible surface area decreases dramatically from 4350 Å^2 to 1489 Å^2 in going from the specific to the nonspecific structure. The DNA remains primarily B form (as in the specific complex), though it is substantially frayed at the ends (Figure 1B). Remarkably, all of the base-specific interactions and DNA backbone contacts are lost. The average temperature factor of the DNA rises from 12 Å^2 to 74 Å^2, suggesting a considerable increase in the mobility of the DNA as it juts out of the widened DNA binding cleft (Figures 1 and 2). The volume of the nonspecific complex rises to 89,790 Å^3 (from 85,960 Å^3 in the specific complex), reflecting the more open configuration on nonspecific DNA binding.

Loss of All Base-Specific and DNA Backbone Contacts

Specific base pair interactions are lost throughout the recognition sequence and not just at the substituted base pair (G*A*ATCC) (Figures 4A and 4B). This total loss of interactions is caused by an increase in the gap between the N-terminal end of the parallel four-helix bundle of BamHI and the major groove surface of the DNA (Figure 2). Most of the amino acids that recognize the cognate sequence (Asn-116, Ser-118, Asp-154, Arg-155, for instance) are located near the amino terminus of this four helix bundle (Newman et al., 1995). For instance, Asn-116 forms hydrogen bonds with both the inner and middle base pairs of the recognition sequence (G*GA*TCC) (Figure 4B), but here it is greater than 8 Å away from these bases, in both the mutant and wild-type half-sites (G*AATC*C). Arg-155 plays a critical role in the specific complex, forming bidentate hydrogen bonds with the guanines of the outer GC base pairs (*G*GATC*C*). However, in the nonspecific complex, despite its length Arg-155 is unable to reach DNA bases across the protein–DNA gap. The volume of this gap or cavity at the protein–DNA interface is 4763 Å^3, as compared to only 282 Å^3 in the specific complex (Kleywegt and Jones, 1994). In general, a gap at the protein–DNA interface would be energetically unfavorable unless it is filled with water molecules. Overall, we detect 89 water molecules at the interface, as compared to 85 in the specific complex. Most of these nonspecific waters have high B factors (average of 43 Å^2), reflecting their mobility as they move in and out of the cavity. However, these waters account for ~78% of the nonspecific cavity volume, which suggests the presence of

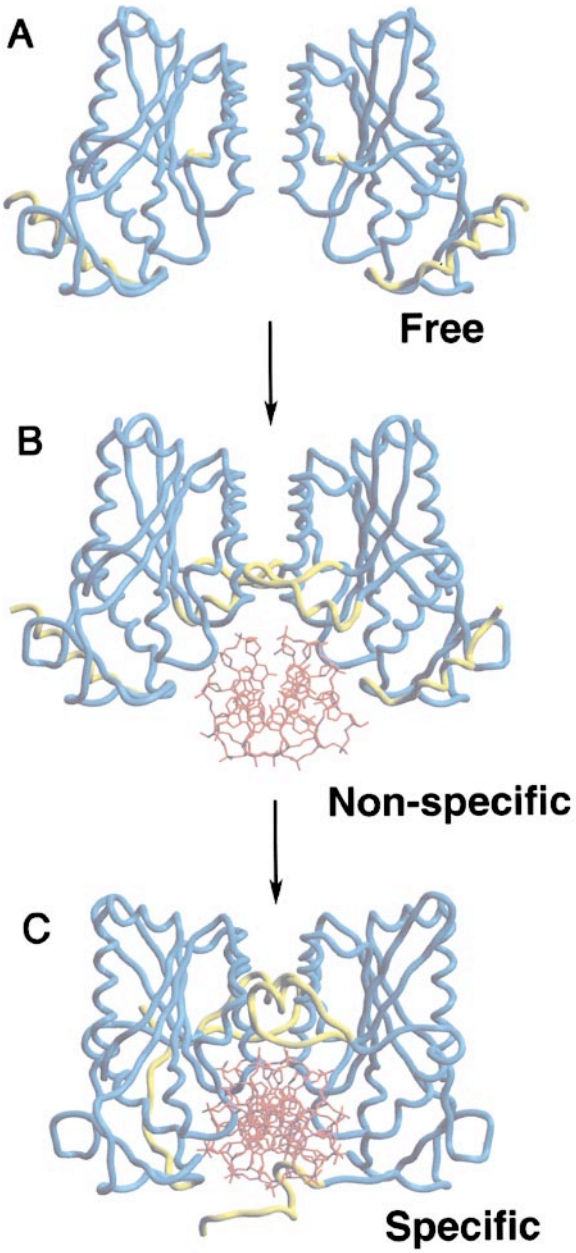

Figure 2. Comparison of BamHI Structures

Structures of free (A), nonspecific (B), and specific (C) DNA-bound forms of BamHI. Regions that undergo local conformational changes are shown in yellow color. The enzyme becomes progressively more closed around the DNA as it goes from the nonspecific to the specific DNA binding mode. Residues 79–92 are unstructured in the free enzyme but become ordered in both the nonspecific and specific DNA complexes, albeit in different conformations. The C-terminal residues unwind in the specific complex to form partially disordered arms, whereas in the nonspecific complex they remain α helical.

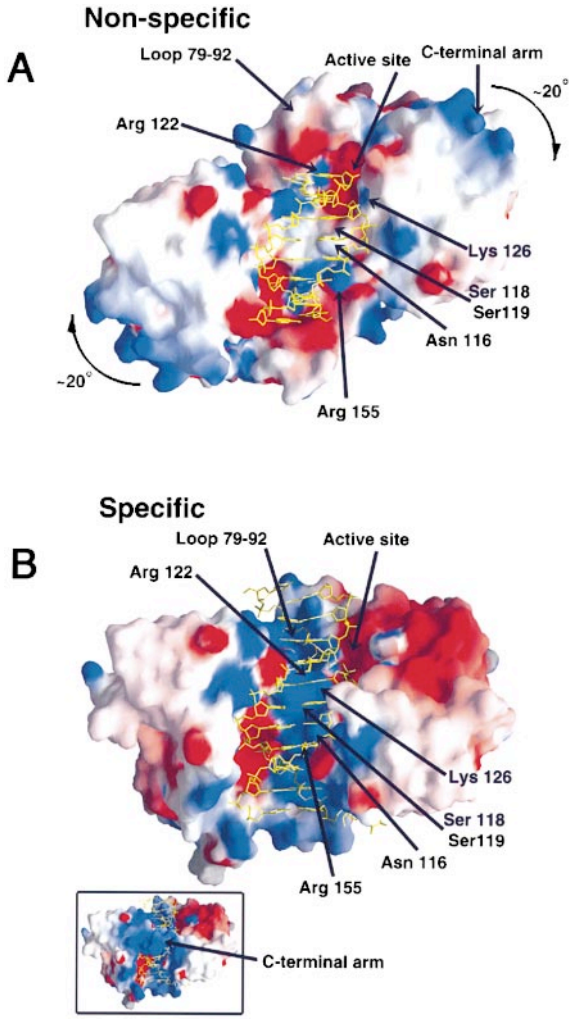

Figure 3. Comparison of Electrostatic Surfaces

The electrostatic surface of BamHI in the nonspecific (A) and the specific complex (B). The red colored areas represent negative electrostatic potential, and the blue areas represent positive potential. Both complexes are viewed down their noncrystallographic two folds with the DNAs oriented vertical. Note the ~20° tilt in the enzyme in going from the nonspecific to the specific binding mode. The specific complex is shown with (inset) and without (main image) the C-terminal arm. The figure was drawn with the aid of program Grasp (Nicholls et al., 1991).

additional water molecules in the cavity but which could not be assigned in our electron density map due to their high mobility. For instance, DNA binding measurements on EcoRI performed under osmotic pressure suggest that the nonspecific complex retains ~110 more water molecules than the specific complex (Sidorova and Rau, 1996). Similar results have been obtained with other DNA binding proteins such as Gal4 repressor and the nonspecific DNA binding protein Sso7d (Garner and Rau, 1995; Lundback et al., 1998).

Local Conformational Changes

The nonspecific BamHI structure is similar to the free enzyme in containing an α helix at the C terminus (residues 194 to 213) (Figure 2). By contrast, in the specific complex, these α helices unfold to form "arms" with the arm from the R subunit fitting into the minor groove and the arm from the L subunit following the DNA sugar-phosphate backbone (Figure 2C). Because these α helices do not unfold in the nonspecific structure, there are

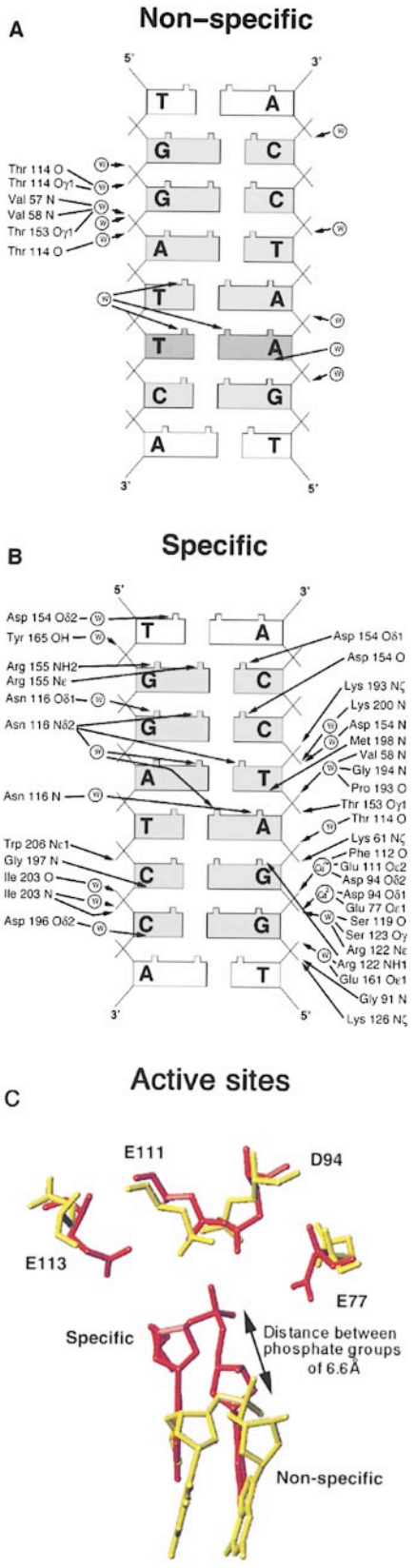

Figure 4. Comparison of Protein–DNA Contacts and Active Sites

(A and B) Summary of protein–DNA contacts in the nonspecific (A) and the specific (B) complexes. The "recognition" sequences are shown in a light shade and the mutated base pair in a dark shade. Arrows represent potential hydrogen bonds, using a distance criteria of <3.2 Å. Circles with W represent water molecules, while the circles with Ca^{2+} represent calcium ions. In the specific complex, the enzyme makes both direct and water-mediated hydrogen bonds with bases in both the major and minor grooves, and contacts with the DNA backbone (shown here for only one subunit). All of these contacts are lost in the nonspecific complex.

(C) Comparison of BamHI active site in the specific (red) and nonspecific (yellow) complexes. The active sites were superimposed using the C_αs of residues Glu-77, Asp-94, Glu-111, and Glu-113. In the nonspecific complex, the active site residues are displaced (>6 Å) away from the scissile phosphodiester.

no minor groove or DNA backbone contacts from these C-terminal residues (Figure 4A). However, since the N termini of these C-terminal α helices are directed toward the DNA backbone, their helix dipole moments will contribute to the stabilization of the nonspecific complex. Thus, the BamHI C-terminal residues may fulfill a dual role: first, as α helices, they may aid in the initial binding and the diffusion of the enzyme on nonspecific DNA; second, by unfolding they may increase the lifetime of the specific complex for the subsequent cleavage reaction.

Strikingly, the segment encompassing residues 79–91 is dragged "down" by the nonspecific DNA as it drops out of the DNA binding cleft, a movement of ~9 Å as compared to the specific complex (Figure 2). The flexibility of this region was evident in the earlier BamHI structures, being disordered in free enzyme but folded in the specific complex (Newman et al., 1994, 1995). The segment adopts a different configuration here and is much more mobile than in the specific complex (C_α average B factor of 41 $Å^2$ versus 23 $Å^2$), reflecting far fewer electrostatic interactions with the DNA backbone.

Mechanism for Achieving Extreme DNA Selectivity

BamHI derives its specificity part from binding and part from catalysis. Single base pair substitutions within the recognition sequence affect binding to a similar extent as a random sequence (Engler, 1998), as in the case of EcoRI (Lesser et al., 1990; Thielking et al., 1990). For instance, the single G:C to A:T base pair change (G*A*ATCC) carries a large energy penalty (11.7 kcal/mol) in forming the activated transition state, with 3.5 kmol/mol due to differences in binding energies in forming the enzyme-DNA complex (E-DNA) and 8.1 kmol/mol due to differences in energies in activating the E-DNA complex to the transition state (Engler, 1998; Jen-Jacobson et al., 2000). The nonspecific structure provides a basis for understanding this extreme selectivity, important in avoiding potentially lethal cleavages at sites that differ by only a single base pair in the bacterial genome. In particular, the outward movement of the BamHI monomers displaces the active site residues (Glu-77, Asp-94, Glu-111, and Glu-113) away from the scissile phosphodiester by greater than 6 Å, with a corresponding loss in metal binding (Figure 4C). By comparison, in the specific complex, the catalytic residues are clustered around the scissile phosphodiester, and together with the nonbridging oxygens of the scissile phosphodiester form a binding site for two divalent cations (Viadiu and Aggarwal, 1998) (Figure 4C). Interestingly, the active site

residues are also displaced in the structure of EcoRV bound across two short DNA oligomers, which mimics a nonspecific complex (Winkler et al., 1993). However, in EcoRV, the displacement of active site residues is due to a change in DNA conformation, whereas in BamHI it is due mostly to an adaptation in protein conformation. At first sight, it seems remarkable that a single base pair change could trigger the conformational changes described above for BamHI. A close inspection of the BamHI structures suggests the loss of hydrogen bonds and steric overlap with two strategically positioned residues (Asn-116 and Asp-154) at the protein–DNA interface (Figure 4B). The introduction of adenine at the second position (G*A*ATCC) will have the effect of disrupting hydrogen bonds Asn-116 makes with both the middle guanine and the inner thymine of the recognition sequence, while the thymine methyl group will cause severe steric clashes with both the main chain and side chain atoms of Glu-154, disrupting the hydrogen bonds Asp-154 makes with the cytosines of both the middle and outer base pairs (*GG*ATCC). Thus, it could be argued that the potential loss of four hydrogen bonds and steric repulsion is sufficient to switch the enzyme to a nonspecific mode of DNA binding, in accordance with similarly observed binding constants on single and multiply mutated DNA sites (Engler, 1998). The symmetrical, outward movement of both BamHI monomers in response to a single base pair change is consistent with the loss of cleavage activity observed at both half-sites (Lesser et al., 1990; Engler, 1998). Taken together, the remarkable complementarity one sees at the BamHI–DNA interface in the specific complex may be a mechanism to ensure that the introduction of even a single wrong base pair leads to a disruption of the interface, thereby forcing the enzyme to dock in a more open mode (Figure 2), which at the same time ends up displacing the active site residues away from the scissile phosphodiesters (Figure 4C). Thus, the enzyme can still bind to the noncognate site (down by $\sim 10^2$ to 10^3) but will rarely cleave it (down by 10^7 to 10^{10}).

Correlation with Studies on Nonspecific DNA Binding and DNA Sliding

Our structural results provide a molecular framework for thermodynamic studies on nonspecific DNA binding. For instance, several calorimetric studies have pointed to the lack of heat capacity change on nonspecific DNA binding (Takeda et al., 1992; Ladbury et al., 1994), in contrast to the large negative heat capacity change observed on specific binding (Spolar and Record, 1994). This is generally taken to indicate a decrease in the solvent-accessible surface area removed from bulk water in nonspecific versus specific DNA binding. Correspondingly, the BamHI nonspecific structure reveals a dramatic decrease in the buried solvent-accessible surface area in going from the specific to the nonspecific state. The enzyme adopts an open configuration that is on the pathway between the free and specifically DNA-bound forms of the enzyme (Figure 2). It has also been suggested that part of the heat capacity change upon specific binding is due to the restriction of soft vibrational modes at the protein–DNA interface (Sturtevant, 1977; Ladbury et al., 1994). The structure fits with this hypothesis, revealing much higher temperature factors at the protein–DNA interface when compared to the specific complex.

Another characteristic of nonspecific DNA binding is its greater sensitivity to salt concentration, when compared to specific binding (deHaseth et al., 1977; Revzin and von Hippel, 1977). This has generally been interpreted in electrostatic terms with suggestions of an alternate nonspecific protein conformation that makes additional DNA backbone contacts (Mossing and Record, 1985; von Hippel and Berg, 1986). Although we see evidence of an alternate BamHI conformation, we also see a loss rather than a gain of DNA backbone contacts. In fact, the nonspecific DNA binding surface is remarkably devoid of positive charge when compared to the specific complex (Figure 3), indicating a major redistribution of charge in going from the nonspecific to the specific DNA binding mode. Much of the electrostatic stabilization of the nonspecific complex appears to arise from the helix dipole moments of several α helices (α4, α6, α7, and their two-fold related counterparts) that project toward the DNA backbone, including the C-terminal α helices that do not unfold on nonspecific DNA binding (Figures 1 and 2).

Like many DNA binding proteins, BamHI can find its target DNA site faster than the three-dimensional diffusion limit and shows an increase in the cleavage reaction as the length of nonspecific DNA around the cognate site is increased (Ehbrecht et al., 1985; Nardone et al., 1986). The nonspecific structure shows how this may occur. The noncognate DNA is bound loosely within a widened DNA binding cleft, making it possible for BamHI to slide along the DNA (Figures 1 and 2). The overall lack of DNA backbone contacts may facilitate diffusion by helping to reduce the lifetime of the nonspecific complex and by lowering the activation energy for the breaking and reforming of DNA contacts as the enzyme moves forward (or backward). All in all, the nonspecific complex provides a snapshot of an enzyme poised for linear diffusion, paving the way for single molecule studies (Guthold et al., 1999) that could address whether the enzyme moves by a corkscrew motion (following the DNA major groove) or along one face of the DNA. The structure provides the most detailed picture yet of how an enzyme selects its cognate site from the multitude of nonspecific sites in a cell.

Experimental Procedures

Crystallization and Data Collection

The nonspecific cocrystals were grown from solutions containing 16%–20% MPD, 10 mM sodium acetate (pH 4.8), and 5 mM $CaCl_2$. The crystals belong to space group $P2_12_12_1$ with unit cell dimensions of a = 114.8 Å, b = 91.1 Å, c = 66.4 Å, $\alpha = 90^\circ$, $\beta = 90^\circ$, $\gamma = 90^\circ$. The presence of DNA in the crystals was confirmed by gel electrophoresis. Three X-ray data sets were measured from cryo-cooled crystals. The first set was measured on an R axis IV imaging plate area detector mounted on a rotating anode X-ray generator, while the second and third sets were measured on an ADSC charge–coupled device detector at the Cornell High Energy Synchrotron Source (CHESS) on beamline A-1 ($\lambda = 0.908$ Å). The HKL program package was used to integrate the X-ray reflections in all three cases (Table 1).

Structure Determination and Refinement

Because the rotating anode data set was the first to become available, it was used to solve the structure by molecular replacement

methods using the program AMoRe (Navaza, 1994). A truncated BamHI subunit (without residues 195–213) taken from the specific complex was used as the initial search model, and the position of the second subunit was found with respect to it. However, attempts to locate the DNA in the electron density map failed at this stage. The program XPLOR (Brunger, 1992) was used to initiate rigid body refinement of the BamHI dimer (20 to 3.5 Å), leaving aside 5% of the reflections for R_{free} calculations. The refinement was continued to the highest resolution shell (2.5 Å) of the rotating anode data by iterative cycles of positional refinement followed by manual rebuilding of the protein using the program O (Jones et al., 1991). B factor refinement was started when the R factor reached ~39%, after which the central six base pairs DNA became better defined in the electron density maps. In addition to the DNA, the loop 72–92 and the C termini of the enzyme were built into the maps. The refinement was extended to 2 Å resolution using the merged data between rotating anode and CHESS-1. At 2 Å resolution, 8 out of 11 base pairs of the DNA could be built, and 373 water molecules (B < 60 Å^2) were assigned. At this stage, the more complete CHESS-2 data set became available and was used to complete the refinement to 1.9 Å resolution, using the CNS package (Brunger et al., 1998). Both anisotropic B factor and bulk solvent corrections were applied to data, and a total of 579 waters (B factors < 65 Å^2) assigned in the electron density map (Table 1).

Structure Analysis

Solvent-accessible surface (SAS) areas were calculated with the program Grasp (Nicholls et al., 1991), using a probe radius of 1.4 Å. The buried SAS area was obtained by first calculating the areas for BamHI and DNA separately, adding them up, and then subtracting the total from the SAS area of the complex. Cavity volumes were calculated in the absence and presence of crystallographically defined water molecules, using the combination of programs Voidoo (Kleywegt and Jones, 1994) and MAMA (Kleywegt and Jones, 1999). Voidoo was used to obtain all the cavity masks corresponding to a rolling probe of radius 1.4 Å, using a grid spacing of 0.3 Å, and MAMA was used to add up all the masks at the protein–DNA interface to give the volume of the final mask.

Acknowledgments

We thank I. Schildkraut for stimulating discussions, R. Kucera for the purified protein, the staff at CHESS and members of the Aggarwal laboratory for help with X-ray data collection, and L. Shapiro for comments on the manuscript. This work was supported by a grant from the National Institutes of Health (A. K. A.). H. V. was supported by a Fulbright/CONACYT scholarship.

Received February 10, 2000; revised March 27, 2000.

References

Brunger, A.T. (1992). X-PLOR Manual. (New Haven, CT: Yale University).

Brunger, A.T., Adams, P.D., Clore, G.M., DeLano, W.L., Gros, P., Grosse-Kunstleve, R.W., Jiang, J.S., Kuszewski, J., Nilges, M., Pannu, N.S., et al. (1998). Crystallography and NMR system: a new software suite for macromolecular structure determination. Acta Crystallogr. D *54*, 905–921.

deHaseth, P.L., Lohman, T.M., and Record, M.T., Jr. (1977). Nonspecific interaction of *lac* repressor with DNA: an association reaction driven by counterion release. Biochemistry *16*, 4783–4790.

Ehbrecht, H.J., Pingoud, A., Urbanke, C., Maass, G., and Gualerzi, C. (1985). Linear diffusion of restriction endonucleases on DNA. J. Biol. Chem. *260*, 6160–6166.

Engler, L.E. (1998). Specificity determinants in the *Bam*HI endonuclease-DNA interaction. PhD thesis, University of Pittsburgh, Pittsburgh, Pennsylvania. pp. 255.

Garner, M.M., and Rau, D.C. (1995). Water release associated with specific binding of gal repressor. EMBO J. *14*, 1257–1263.

Guthold, M., Zhu, X., Rivetti, C., Yang, G., Thomson, N.H., Kasas, S., Hansma, H.G., Smith, B., Hansma, P.K., and Bustamante, C. (1999). Direct observation of one-dimensional diffusion and transcription by *Escherichia coli* RNA polymerase. Biophys. J. *77*, 2284–2294.

Harrison, S.C., and Aggarwal, A.K. (1990). DNA recognition by proteins with the helix-turn-helix motif. Annu. Rev. Biochem. *59*, 933–969.

Jen-Jacobson, L., Engler, L.E., Ames, J.T., Kurpiewski, M.R., and Grigorescu, A. (2000). Thermodynamic parameters of specific and nonspecific protein–DNA binding. Supramolecular Chemistry, in press.

Jones, T.A., Zou, J.Y., and Cowan, S.W. (1991). Improved methods for building models in electron density maps and the location of errors in these models. Acta Crystallogr. A *47*, 110–119.

Kleywegt, G.J., and Jones, T.A. (1994). Detection, delineation, measurement and display of cavities in macromolecular structures. Acta Crystallogr. D *50*, 178–185.

Kleywegt, G.J., and Jones, T.A. (1999). Software for handling macromolecular envelopes. Acta Crystallogr. D *55*, 941–944.

Ladbury, J.E., Wright, J.G., Sturtevant, J.M., and Sigler, P.B. (1994). A thermodynamic study of the *trp* repressor-operator interaction. J. Mol. Biol. *238*, 669–681.

Lesser, D.R., Kurpiewski, M.R., and Jen-Jacobson, L. (1990). The energetic basis of specificity in the *Eco*RI endonuclease-DNA interaction. Science *250*, 776–786.

Lundback, T., Hansson, H., Knapp, S., Ladenstein, R., and Hard, T. (1998). Thermodynamic characterization of non-sequence-specific DNA-binding by the Sso7d protein from *Sulfolobus solfataricus*. J. Mol. Biol. *276*, 775–786.

Mossing, M.C., and Record, M.T., Jr. (1985). Thermodynamic origins of specificity in the *lac* repressor-operator interaction. Adaptability in the recognition of mutant operator sites. J. Mol. Biol. *186*, 295–305.

Nardone, G., George, J., and Chirikjian, J.G. (1986). Differences in the kinetic properties of *Bam*HI endonuclease and methylase with linear DNA substrates. J. Biol. Chem. *261*, 12128–12133.

Navaza, J. (1994). AMoRe: an automated package for molecular replacement. Acta Crystallog. A *50*, 157–163.

Newman, M., Strzelecka, T., Dorner, L.F., Schildkraut, I., and Aggarwal, A.K. (1994). Structure of restriction endonuclease *Bam*HI and its relationship to *Eco*RI. Nature *368*, 660–664.

Newman, M., Strzelecka, T., Dorner, L.F., Schildkraut, I., and Aggarwal, A.K. (1995). Structure of *Bam*HI endonuclease bound to DNA: partial folding and unfolding on DNA binding. Science *269*, 656–663.

Nicholls, A., Sharp, K.A., and Honig, B. (1991). Protein folding and association: insights from the interfacial and thermodynamic properties of hydrocarbons. Proteins *11*, 281–296.

Pabo, C.O., and Sauer, R.T. (1992). Transcription factors: structural families and principles of DNA recognition. Annu. Rev. Biochem. *61*, 1053–1095.

Revzin, A., and von Hippel, P.H. (1977). Direct measurement of association constants for the binding of *Escherichia coli lac* repressor to non-operator DNA. Biochemistry *16*, 4769–4776.

Roberts, R.J., and Halford, S.E. (1993). Type II restriction endonucleases. In Nucleases, S.M. Linn, R.S. Lloyd, and R.J. Roberts, eds. (Cold Spring Harbor, NY: Cold Spring Harbor Laboratory Press), pp. 35–88.

Sidorova, N.Y., and Rau, D.C. (1996). Differences in water release for the binding of *Eco*RI to specific and nonspecific DNA sequences. Proc. Natl. Acad. Sci. USA *93*, 12272–12277.

Spolar, R.S., and Record, M.T., Jr. (1994). Coupling of local folding to site-specific binding of proteins to DNA. Science *263*, 777–784.

Sturtevant, J.M. (1977). Heat capacity and entropy changes in processes involving proteins. Proc. Natl. Acad. Sci. USA. *74*, 4749–4751.

Takeda, Y., Ross, P.D., and Mudd, C.P. (1992). Thermodynamics of *Cro* protein–DNA interactions. Proc. Natl. Acad. Sci. USA *89*, 8180–8184.

Thielking, V., Alves, J., Fliess, A., Maass, G., and Pigoud, A. (1990). Accuracy of the *Eco*RI restriction endonuclease: binding and cleavage studies with oligodeoxynucleotide substrates containing degenerate recognition sequences. Biochemistry *29*, 4682–4691.

Viadiu, H., and Aggarwal, A.K. (1998). The role of metals in catalysis by the restriction endonuclease *Bam*HI. Nat. Struct. Biol. *5*, 910–916.

Viadiu, H., Kucera, R., Schildkraut, I., and Aggarwal, A.K. (2000). Crystallization of restriction endonuclease *Bam*HI with non-specific DNA. J. Struct. Biol., in press.

von Hippel, P.H. (1994). Protein–DNA recognition: new perspectives and underlying themes. Science *263*, 769–770.

von Hippel, P.H., and Berg, O.G. (1986). On the specificity of DNA–protein interactions. Proc. Natl. Acad. Sci. USA *83*, 1608–1612.

von Hippel, P.H., and Berg, O.G. (1989). Facilitated target location in biological systems. J. Biol. Chem. *264*, 675–678.

Winkler, F.K., Banner, D.W., Oefner, C., Tsernoglou, D., Brown, R.S., Heathman, S.P., Bryan, R.K., Martin, P.D., Petratos, K., and Wilson, K.S. (1993). The crystal structure of *Eco*RV endonuclease and of its complexes with cognate and non-cognate DNA fragments. EMBO J. *12*, 1781–1795.

Protein Data Bank ID Code

Coordinates have been deposited in the Protein Data Bank (code 1ESG).